

## Use of brGDGTs in surface geochemical exploration for petroleum —A case study of oil and gas fields in the Jiyang depression

ZHOU HaoDa<sup>1,2,3</sup>, HU JianFang<sup>1\*</sup>, XIONG YongQiang<sup>1</sup> & LIANG QianYong<sup>1,2</sup>

<sup>1</sup>State Key Laboratory of Organic Geochemistry, Guangzhou Institute of Geochemistry, Chinese Academy of Sciences, Guangzhou 510640, China;

<sup>2</sup>Graduate University of Chinese Academy of Sciences, Beijing 100049, China;

<sup>3</sup>Zhuhai Central Station of Marine Environmental Monitoring, State Oceanic Administration, Zhuhai 519015, China

Received June 29, 2013; accepted November 25, 2013; published online April 25, 2014

Branched glycerol dialkyl glycerol tetraethers (brGDGTs), likely produced by bacteria in soil and peat, are widely distributed, easily detected, newly adopted biomarker compounds. In this study, brGDGTs were used to explore the relationship between the absolute abundance of brGDGTs and the distribution of oil and gas fields in the Duoshiqiao area of the Jiyang depression. The results showed that the concentrations at the Xiakou fault and in the oil and gas fields were obviously higher than those in the contrast areas. The clear relationship among the concentration of brGDGTs, the distribution of oil and gas fields, and the acidolysis hydrocarbon (ethane) indicates that the concentration effectively responds to hydrocarbon seeps from the oil and gas field below. brGDGTs may become some of the most important indicators in surface geochemical prospecting for oil and gas.

**brGDGTs, Jiyang depression, surface seep, geochemical exploration, petroleum**

**Citation:** Zhou H D, Hu J F, Xiong Y Q, et al. 2014. Use of brGDGTs in surface geochemical exploration for petroleum—A case study of oil and gas fields in the Jiyang depression. *Science China: Earth Sciences*, 57: 1605–1612, doi: 10.1007/s11430-014-4856-x

Large amounts of data indicate that hydrocarbons generated and trapped at various depths leak to the surface in varying but detectable quantities (Schumacher, 1999; Saunders et al., 1999). Over the past several decades, few have questioned the fact that hydrocarbons migrate to the near-surface and surface in detectable amounts. Vertical percolation of hydrocarbons is the theoretical basis of surface geochemical exploration for oil and gas. The hydrocarbons interact with various kinds of near-surface mediums, such as rocks, pore water, soil particles, and groundwater. Some of the hydrocarbons are stored in different forms by near-surface soil, changing the original soil and vegetation (Jiang et al., 2003). Geochemical prospecting consists in searching at the surface or near-surface for hydrocarbons from deep sources,

based on their alterations to chemical characteristics such as the concentrations or isotopic abundances of light hydrocarbons (principally C<sub>1</sub>–C<sub>5</sub> alkanes) or high-molecular-weight hydrocarbons (such as 2–4 ring aromatics).

Furthermore, the abundance of hydrocarbon-oxidizing microbes is expected to change in the soil and sediment overlying an oil and gas reservoir (Schumacher, 1999). Microbial exploration is a new cross-discipline development in surface geochemical exploration technology. It combines geochemical and microbial research to correlate near-surface microbiological soil anomalies with deep underground reservoirs. At the beginning of oil and gas exploration, microbial prospecting can be economic and effective for selecting exploration blocks in order to reduce the risk (Hanson et al., 1996; Matthew, 1996). The principle of microbial prospecting technology is as follows: hydrocarbon gas continuously undergoes vertical diffusion and migrates towards the sur-

\*Corresponding author (email: hujf@gig.ac.cn)

face driven by reservoir pressure; the microorganisms in the soil above the reservoir then consume this hydrocarbon gas as their only energy source, which is abnormal (Schumacher, 1999; Nazina, 2000; Wu, 2005). At present, the bacteria mainly associated with microbial prospecting are methane-oxidizing bacteria and other hydrocarbon-oxidizing bacteria (Mei et al., 2004).

Because of its advantages, microbiological technology has received attention from explorers as a new method for surface identification of oil and gas. However, extensive application of the technology has been negatively affected by the long process cycle, high specialization, and methane source of the traditional microbial technique for oil and gas exploration (Yuan et al., 2002; Hu et al., 2006).

Figure 1 shows the molecular structure of branched glycerol dialkyl glycerol tetraethers (brGDGTs), which are generally believed to be produced by certain bacteria that are widely distributed in soil, peat, and lake settings (Weijers et al., 2007a; 2009). The bacteria that are the origins of brGDGTs are sensitive to environmental factors (such as

temperature and pH). brGDGTs are often used to reconstruct the paleoclimate of a land system on the basis of distributions that adjust with the environment (Weijers et al., 2007b; 2007c). Some researches suggest that brGDGTs are derived from *Acidobacteria* (Sinninghe Damsté et al., 2011; Weijers et al., 2009). One of metabolic patterns of gaseous hydrocarbon by microbial, the gaseous hydrocarbon, containing two to four carbon is first metabolized to acetate (Atlas, 1991). Bacteria producing brGDGTs may be associated with gaseous hydrocarbon metabolites: acetate. In the present study, the abundance and distribution of brGDGTs were measured in the Jiyang depression to explore the application of such measurements in surface geochemical exploration for oil and gas.

## 1 Sampling and methods

### 1.1 Study area and sampling

The study area (Figure 2) is located at the borders of Linyi,

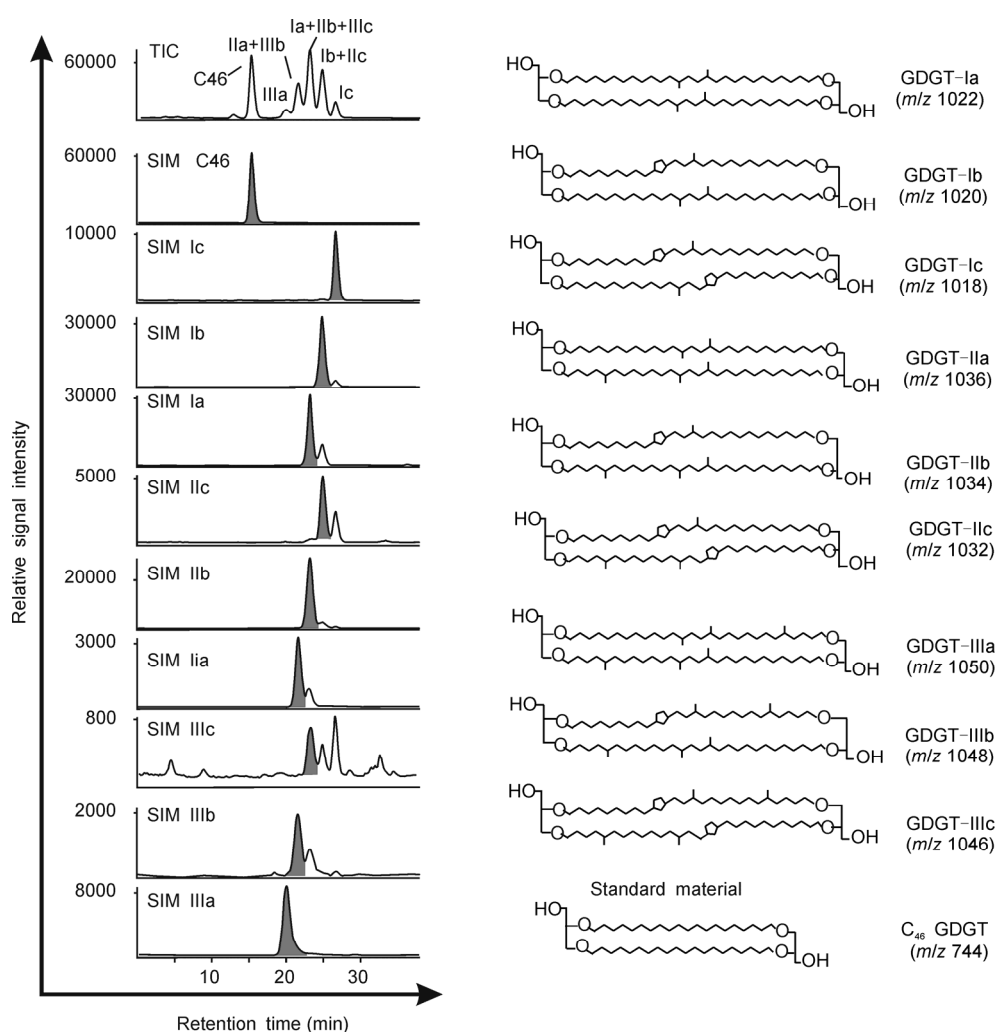


**Figure 1** HPLC/MS base peak chromatograms and mass chromatograms of the different brGDGTs and corresponding structures.

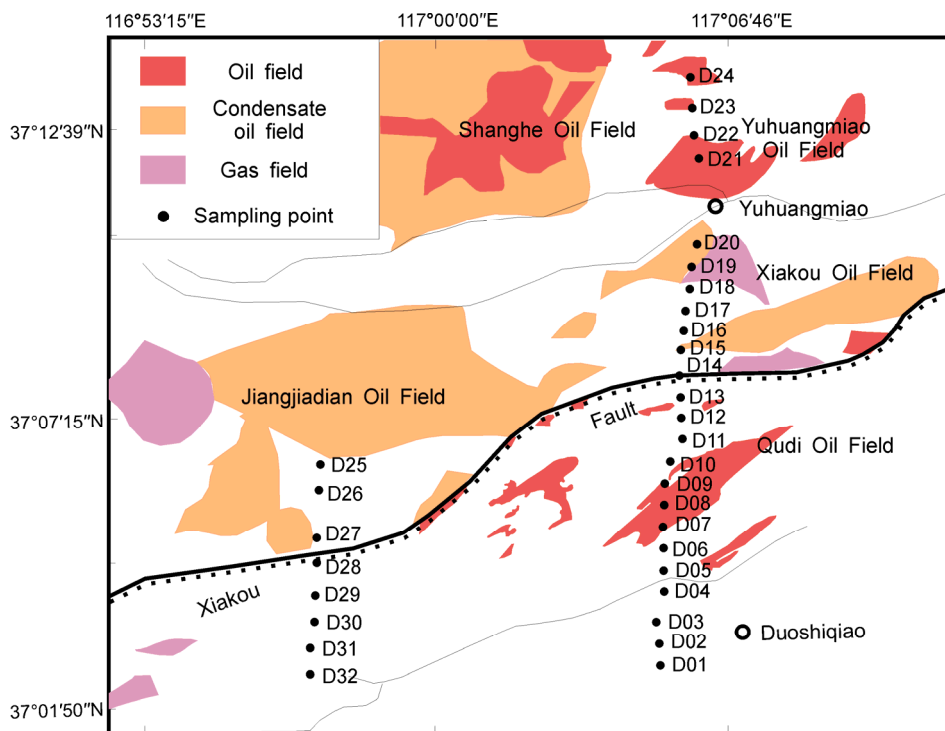


**Figure 2** Study area and sampling points.

Jiyang, and Shanghe counties in the north of Jinan, Shandong Province. The area lies in the southwest region of the Huimin sag and is associated with the Linnan subsag in the south, the Qudi horst in the middle, and the Jiyang subsag in the north. The oil stratum is the main Tertiary Shahejie Formation, existing in the Upper Paleozoic coal strata, where a fault structure is evident (Chen et al., 2005). The fault traversing the area is the Xiakou fault, which is the secondary fault dividing the Linnan subsag and the Linnan slope (Du, 2005; Zhao et al., 2000).

Because the sampling area belongs to farmland, any disturbance of the surface soil is serious. The root systems of weeds and crops generally find it difficult to attain depths of more than 100 cm in the surface soil. However, the physical and chemical properties of the soil below 100 cm depth are similar, with relatively uniform nutrition, so the soil at 150 cm depth was sampled. As shown in Figure 2, a total of 32 sampling points were selected from north to south, with 28 points throughout the oil and gas field and 4 blank points in the contrast area (D29–D32). There was no oil and gas distribution in the contrast area, because of the sealing effect of the Xiakou fault (Gao et al., 2003).

## 1.2 Methods

### 1.2.1 Sample pretreatment method

Samples for lipid analysis were freeze dried and then powdered with a mortar and pestle before extraction. Approximately 500 mg of freeze-dried sample, with a moderate

amount of C<sub>46</sub>-GDGT, underwent Soxhlet extraction with dichloromethane (DCM) and methanol (MeOH) (2:1, v/v) for 72 h. The solvent was evaporated and the extract was separated by Al<sub>2</sub>O<sub>3</sub> column chromatography with hexane/DCM (9:1, v/v) and DCM/MeOH (1:1, v/v) as sequential eluents. The polar fraction (DCM/MeOH) was concentrated by rotary evaporation, redissolved in hexane/isopropanol (99:1, v/v), and filtered using a 0.45- $\mu$ m PTFE filter. The filtrate was tested by high-performance liquid chromatography atmospheric pressure chemical ionization mass spectrometry (HPLC/APCI-MS).

The total organic carbon (TOC) analysis was performed by taking samples of about 1 g, adding 10% hydrochloric acid for 24 h to remove carbonate, drying the samples under a condition of 60°C, and measuring the C content with an IsoPrime vario MICRO cube elemental analyzer (accuracy  $\pm 0.5\%$ ).

### 1.2.2 Instrumental method

The HPLC/MS method used was modified from that described by Hopmans et al. (2000) as discussed by Schouten et al. (2006).

(1) Chromatography conditions. Analyses were performed using an Agilent 1200 Series liquid chromatograph equipped with an auto-injector and ChemStation chromatography management software. Separation was effected with a Pre-vail Cyano column (2.1 mm $\times$ 150 mm, 3  $\mu$ m; Alltech, Deerfield, USA) maintained at 30°C. The injection volume was 3  $\mu$ L. GDGTs were eluted isocratically with 99% hexane

and 1% propanol for 5 min, followed by a linear gradient to 2% propanol over 40 min. The flow rate was 0.2 mL min<sup>-1</sup>. After each analysis, the column was backflushed with hexane/propanol (90:10, v/v) at 0.2 mL min<sup>-1</sup> for 15 min.

(2) Mass spectrometry conditions. Detection was achieved with an Agilent 6410 triple quadrupole mass spectrometer (APCI-MS) using positive-ion chemical ionization under atmospheric pressure. The conditions were as follows: nebulizer pressure 60 psi; vaporizer temperature 400°C; drying gas N<sub>2</sub>, flow rate 5 L min<sup>-1</sup>, temperature 200°C; capillary voltage 2500 V; and corona current 5 μA. GDGTs were detected by single-ion monitoring (SIM) of their [M+H]<sup>+</sup> and [M+H]<sup>+</sup>+1 (i.e., protonated molecular ions and first isotope peak ions) and were quantified by integration of the peak areas. Figure 1 shows values of *m/z*.

## 2 Results and discussion

### 2.1 Distribution of brGDGTs

brGDGT compounds were detected in all samples (Figure 1), with a total concentration of 4.0–4.0 ng g<sup>-1</sup>. The concentrations of I, II, and III were 1.8–32.7, 1.8–33.0, and 0.5–7.3 ng g<sup>-1</sup>, respectively (Table 1). The distribution of brGDGTs at various points was similar, with Ia, Ib, IIa, and IIb dominant and GDGT-III content relatively minimal (3%–16%). The concentrations tended to decrease as the number of cyclopentane groups in the brGDGTs changed from zero to two. In all samples the average percentage content by compound was 50% for class a, 40% for class b, and 10% for class c (Figure 3). These characteristics are similar to those of brGDGTs in other parts of the soil (Weijers et al., 2007a;

**Table 1** brGDGT concentration of each sample

Sites	brGDGTs Concentrations (ng g <sup>-1</sup> )													Total	TOC
	Ic	Ib	Ia	Total of I	IIc	IIb	IIa	Total of II	IIIc	IIb	IIIa	Total of III			
D01	0.7	1.6	1.6	3.9	0.3	1.7	1.7	3.7	0.1	0.2	0.7	0.9	8.6	0.20	
D02	0.7	1.3	2.2	4.2	0.3	2.6	2.9	5.8	0.2	0.3	1.4	1.9	12.0	0.07	
D03	0.8	2.6	2.7	6.0	0.4	2.6	3.6	6.7	0.1	0.4	1.9	2.4	15.1	0.27	
D04	0.5	1.4	1.3	3.2	0.3	1.6	1.3	3.2	0.1	0.2	0.5	0.7	7.1	0.15	
D05	1.4	5.6	5.7	12.7	0.7	4.9	7.5	13.1	0.1	0.5	2.8	3.4	29.2	0.41	
D06	1.1	2.9	2.8	6.8	0.4	2.1	2.3	4.8	0.1	0.2	0.6	0.9	12.5	0.38	
D07	1.0	1.7	1.2	4.0	0.4	1.6	1.0	3.0	0.1	0.2	0.4	0.6	7.6	0.13	
D08	1.8	6.0	6.2	14.0	0.5	4.5	6.7	11.7	0.1	0.4	2.0	2.5	28.2	0.43	
D09	1.3	4.6	5.3	11.2	0.8	5.1	7.6	13.6	0.2	0.5	3.1	3.7	28.5	0.39	
D10	1.7	5.2	5.9	12.8	0.9	5.5	8.6	15.1	0.2	0.6	3.4	4.1	32.0	0.42	
D11	2.1	9.3	8.9	20.2	0.9	10.0	15.1	25.9	0.2	0.9	5.9	7.0	53.1	0.45	
D12	1.6	5.9	5.3	12.8	0.9	5.6	6.0	12.6	0.2	0.7	1.9	2.8	28.1	0.30	
D13	1.9	6.9	6.3	15.0	0.9	7.6	7.8	16.3	0.2	0.8	3.2	4.3	35.6	0.40	
D14	4.1	15.3	13.3	32.7	2.3	14.3	16.4	33.0	0.3	1.3	5.7	7.3	73.0	0.46	
D15	1.3	4.7	4.8	10.8	0.7	4.8	5.9	11.4	0.1	0.5	2.3	3.0	25.2	0.27	
D16	1.5	4.6	4.7	10.8	0.9	4.9	5.1	10.9	0.2	0.5	2.0	2.6	24.3	0.34	
D17	1.6	2.6	2.3	6.5	1.0	3.7	2.9	7.6	0.3	0.6	1.3	2.2	16.3	0.15	
D18	0.9	1.5	1.3	3.6	0.5	1.9	1.4	3.7	0.1	0.2	0.6	0.9	8.3	0.11	
D19	0.6	1.4	1.3	3.2	0.3	1.9	1.3	3.5	0.1	0.2	0.6	0.9	7.6	0.14	
D20	1.2	2.9	2.7	6.9	0.6	3.2	2.6	6.4	0.1	0.3	1.0	1.4	14.7	0.12	
D21	1.7	3.2	3.4	8.4	0.9	4.0	3.1	8.0	0.2	0.5	1.4	2.1	18.5	0.18	
D22	1.9	4.9	4.3	11.1	0.7	4.0	3.6	8.3	0.1	0.3	1.1	1.5	20.8	0.24	
D23	1.9	3.5	3.6	8.9	0.8	3.5	3.1	7.4	0.2	0.4	1.0	1.6	17.9	0.37	
D24	2.5	5.6	5.7	13.7	0.9	4.7	4.9	10.5	0.2	0.4	1.5	2.1	26.3	0.30	
D25	0.6	1.6	1.7	3.9	0.3	1.7	1.6	3.7	0.1	0.2	0.5	0.7	8.3	0.26	
D26	1.9	5.3	5.1	12.4	0.9	5.1	5.9	11.9	0.1	0.4	1.9	2.5	26.8	0.13	
D27	0.6	1.4	1.5	3.6	0.3	1.7	1.8	3.9	0.0	0.2	0.6	0.9	8.3	0.16	
D28	2.3	9.8	10.2	22.4	1.3	9.0	21.5	31.8	0.2	0.6	6.5	7.2	61.4	0.28	
D29	0.5	0.7	0.6	1.8	0.3	0.9	0.6	1.8	0.1	0.1	0.3	0.5	4.0	0.05	
D30	1.0	2.8	2.9	6.7	0.3	2.1	2.4	4.8	0.1	0.2	0.7	0.9	12.5	0.29	
D31	0.7	1.1	1.2	3.0	0.3	1.3	1.2	2.8	0.0	0.2	0.4	0.6	6.3	0.16	
D32	1.3	1.9	1.9	5.0	0.6	2.2	2.0	4.9	0.1	0.2	0.7	1.1	11.0	0.19	
mean	1.4	4.1	4.0	9.4	0.7	4.1	5.0	9.7	0.1	0.4	1.8	2.3	21.5	0.26	

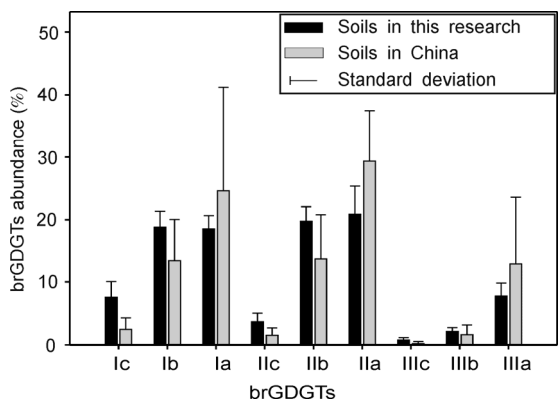


**Figure 3** Average percentage of brGDGTs. Black column: samples in this research; gray column: soils in China (Yang et al., 2012).

Sun et al., 2011; Yang et al., 2012).

As shown in Figure 4, the total brGDGT concentration was generally low in the blank contrast area but rose markedly in the oil and gas area. There was also rising of the brGDGT concentration at the Xiakou fault, presumably resulting from its dual conducting and sealing function (Zhu et al., 2009; Zhao et al., 2000). In fact, the highest levels of brGDGTs were at D14 and D28, which lay on the Xiakou fault near the centerline of the Linnan subsag and hence the oil source. Both oil and gas readily migrate to the surface along the fault (Fu et al., 2002; Cai, 2008), so oil and gas seepage at D14 and D28 may be greater than at other sampling points. The concentration of brGDGTs was higher at D05 than at the adjacent sampling points. This sampling

point is located at the split in the Qudi fault at the edge of the oilfield. Again, oil and gas leakage can occur along the fault, making the location of surface leakage differ from the area overlying the reservoir, as really observed in many oilfields (Jia, 2000). Hence, oil and gas leaks at D05 may be greater than at the adjacent sampling points. The box figure in the statistical analysis clearly shows that the brGDGT content in the oil and gas areas and on the Xiakou fault is significantly higher than that in the blank contrast area (Figure 5). Specifically, the brGDGT content in the blank area is one-third of that in the oil and gas areas and one-eighth of that on the Xiakou fault.

The study area was divided into four areas by the Xiakou fault: A (D01–D13), B (D15–D24), C (D25–D27), and D (D29–D32). The brGDGT content had different characteristics in A, B, C, and D: it was highest in A, with a maximum of 53.11 ng g<sup>-1</sup> (at D11), minimum of 7.13 ng g<sup>-1</sup> (at D04), and mean of 22.89 ng g<sup>-1</sup>; it was lower in B than in A, with a maximum of 26.26 ng g<sup>-1</sup> (at D24), minimum of 7.59 ng g<sup>-1</sup> (at D19), and mean of 17.97 ng g<sup>-1</sup>; and it was higher in C than in D, with a maximum of 26.76 ng g<sup>-1</sup> (at D26), minimum of 8.32 ng g<sup>-1</sup> (at D27), and mean of 14.47 ng g<sup>-1</sup>. The brGDGT content in A, B, and C was 3, 2, and 2 times higher than that in the blank area, respectively. In the middle of the Xiakou fault, there is a good channel for hydrocarbon migration; thus, oil and gas from the Linnan sag passed over the Xiakou fault to the Linnan slope zone and formed the Qudi Oil Field in A. The reservoir is buried shallower in A than in B, so leakage of the hydrocarbons to the surface soil

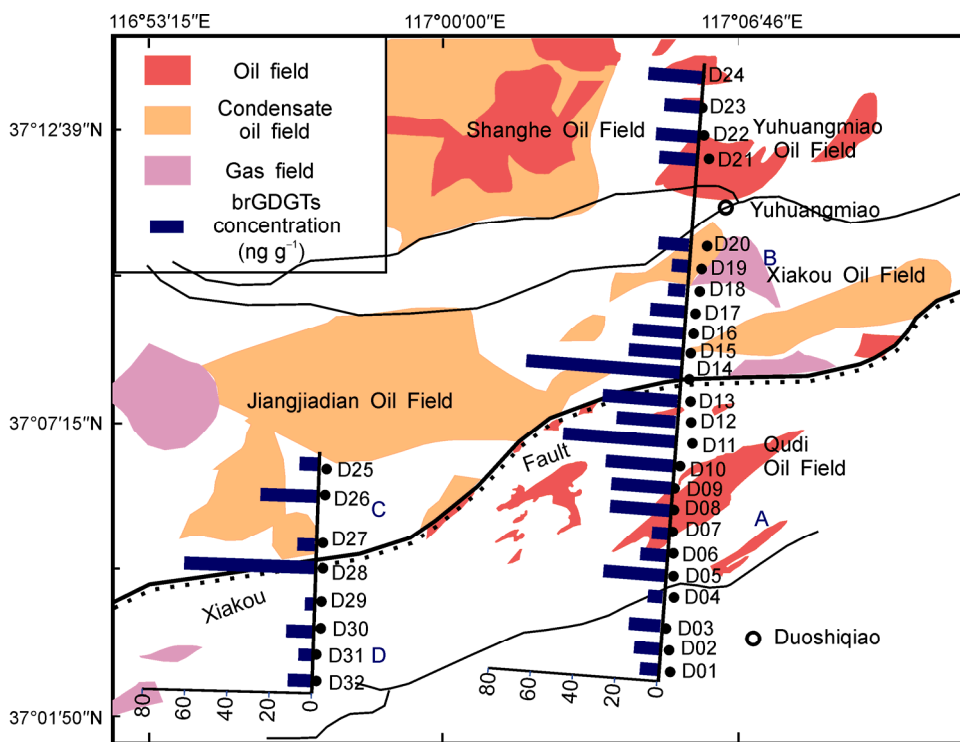


**Figure 4** brGDGT concentrations in the study area (unit: ng g<sup>-1</sup>). In the column charts, X and Y axes indicate sampling points and brGDGTs concentrations of corresponding samples, respectively.

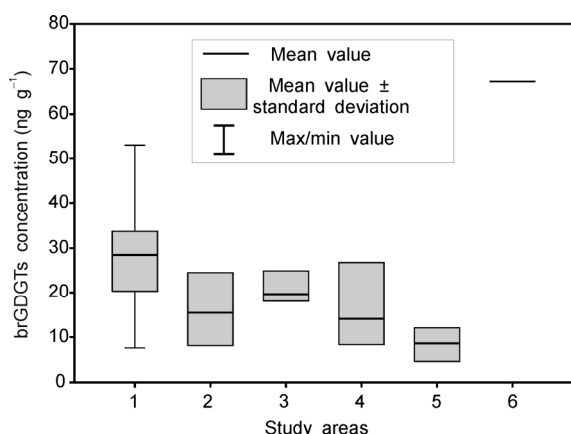


**Figure 5** Box plot of brGDGT concentrations. 1: Qudi Oil Field; 2: Xiakou Oil Field; 3: Yuhuangmiao Oil Field; 4: Jiangjiadian Oil Field; 5: blank area; 6: Xiakou fault.

was easier in A than in B. At the southwest part of the Xiakou fault, the good sealing ability blocked hydrocarbon migration from the Linnan sag to the Linnan slope zone; thus, the Linnan Oil Field formed in the footwall of the fault, with little hydrocarbon seepage. There are no reservoirs in D and no leakages of hydrocarbons to the surface soil. In this study, D was selected as the blank contrast area (Du, 2005; Gao et al., 2003; Han et al., 2003).

The sampling points located on top of the oil and gas fields would have been affected by vertical seepage of the oil and gas. Such leakage of hydrocarbons can promote the production of brGDGTs through microbial proliferation,

and brGDGT content can indicate the underlying oil and gas seepage.

To remove the influence of sample composition on brGDGT content, the brGDGT concentration of each sample was normalized to TOC. The results indicated that the overall trend in the spatial distribution of the brGDGTs was unchanged. Figure 6 shows that the brGDGT content at the Xiakou fault and in the oil and gas area was higher than that in the blank area. However, at certain sampling points, such as D07 and D17–D20 in the Qudi and Xiakou Oil Fields, the relative brGDGT content rose, which emphasized the effect of vertical leakage of hydrocarbons in oil and gas areas.

## 2.2 Comparison with other geochemical indices

The distributions of brGDGT concentration and acidolysis hydrocarbon concentration (ethane concentration, unpublished data) exhibited moderate consistency in oil and gas areas (Figure 7 has  $R^2=0.47$  if D14 and D28 at the Xiakou fault are removed). High values of brGDGT content and ethane content both appeared in the Qudi Oil Field (including the Qudi fault zone), the Yuhuangmiao Oil Field, and the Jiangjiadian oilfield, which showed that both kinds of geochemical exploration indicator can reveal the existence of the reservoir. However, the two indicators gave inconsistent responses at the fault zone: relatively high brGDGTs content was detected at two points on the Xiakou fault (D14 and D28), while acidolysis hydrocarbon concentrations were

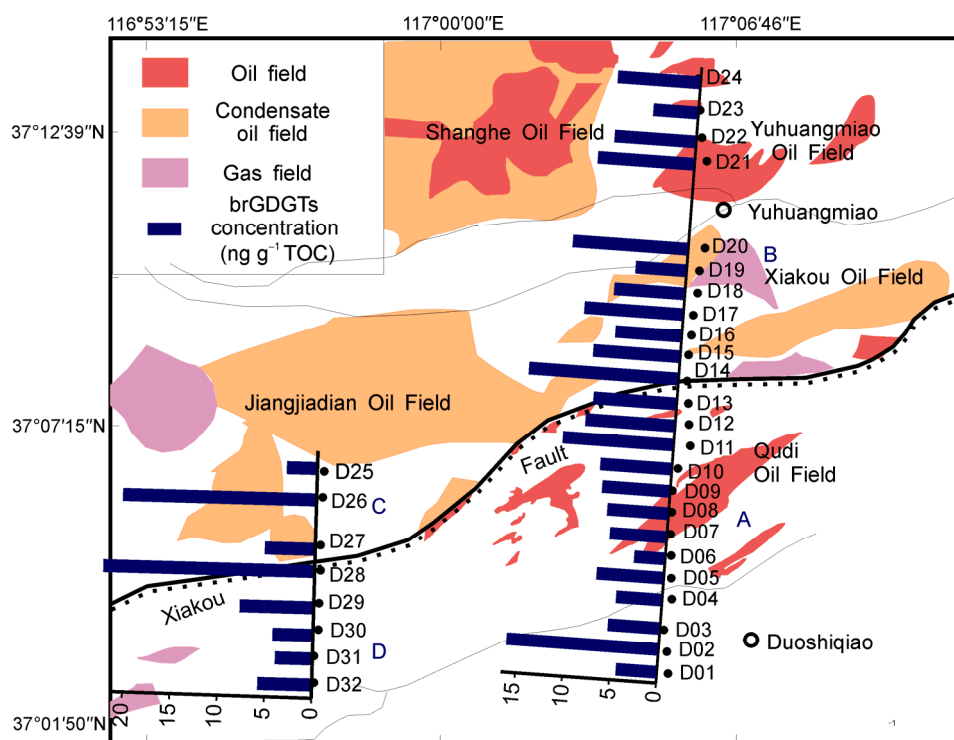


**Figure 6** brGDGT content normalized to TOC in the study area (unit:  $\mu\text{g g}^{-1}$  TOC). In the column charts, X and Y axes indicate sampling points and brGDGTs concentrations of corresponding samples, respectively.

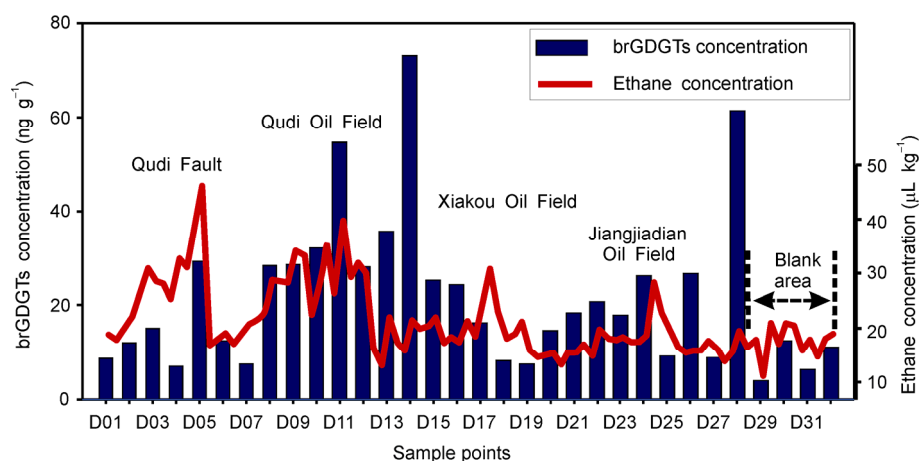


**Figure 7** Distributions of brGDGT and acidolysis hydrocarbon (ethane) concentrations.

relatively low and thus indicated no significant abnormality.

Hydrocarbons migrated from the deep reservoir to the near-surface soil by leakage and were partly saved there in the form of free, physical, and chemical adsorption as well as gas-liquid inclusions and so on. Moreover, all kinds of hydrocarbon gas were balanced through exchanging functions. For example, when the free hydrocarbon gas in pores decreased, weakly adsorbed hydrocarbons were released to maintain the dynamic balance of the soil gas. Thus, hydrocarbon gas obviously leaked upward along the Xiakou fault, perhaps because the bottom of the fault was connected with the center of a hydrocarbon source during the early period of the Linnan depression. At the same time, hydrocarbons promoted the quantity and activity of bacteria, producing brGDGTs that are recorded in the sediment as molecular brGDGTs in fossils. Since the middle of the Tertiary, the activities of Xiakou fault have gradually weakened and the plugging function has increased (Ning et al., 2008). The area developed a shortage of oil, causing a gradual loss of the hydrocarbons trapped in carbonates and other secondary minerals (Heroy, 1969), until the concentration finally decreased to the background value. Hence, the acidolysis hydrocarbon index (ethane content) disclosed no obvious abnormalities at the Xiakou fault zone. The headspace gas method extracted no hydrocarbon gases from these regions, which also supports this point.

The results above show that both the brGDGT index and the acidolysis hydrocarbon index respond well to hydrocarbon gas leakage from underlying oil and gas fields. The high correlation ( $R^2=0.47$ ) of the brGDGT content and the ethane content in soil samples further supports the concept of biological brGDGT sources related to oil and gas, so brGDGT content presumably can be used as an alternative indicator of hydrocarbon gas leakage. In addition, compared to the acidolysis hydrocarbon index, the brGDGT indicator produced by bacteria in a process of gradual accumulation is more stable (Schouten et al., 2008; Ménot et al., 2006; Schouten et al., 2013) and could record a history of hydro-

carbon seepage.

### 3 Discussion

The brGDGT content derived from bacteria in the soil of the Jiyang depression was higher in the oil and gas areas and fault zone than in the blank contrast area, implying that the brGDGT content is possibly a response to oil and gas leakage from the underlying reservoir. The brGDGT index and acidolysis hydrocarbon index exhibited good consistency in the oil and gas areas, indicating that brGDGTs may provide a new criterion for surface geochemical exploration for oil and gas.

*This work was supported by the Knowledge Innovation Program of the Chinese Academy of Sciences (Grant No. KZCXZ-YW-JC103). This is also contribution no.1866 from Guangzhou Institute of Geochemistry, Chinese Academy of Sciences.*

- Atlas R M. 1991. Petroleum Microbiology. Beijing: Petroleum Industry Press. 107
- Cai Y X. 2008. Characteristics of fault developed in Jiyang sag and its control over hydrocarbon migration and accumulation (in Chinese). *Nat Gas Geosci*, 19: 56–61
- Chen H Y, Yu J G, Shu L S, et al. 2005. The structural styles and their relation with petroleum-gas resources of the Jiyang depression, Shandong Province, China (in Chinese). *Geol J Chin Uiver*, 11: 622–632
- Du Y M. 2005. Effect of Xiakou fault on field distribution and petroleum migration in Linnan slope area (in Chinese). *Xinjiang Petrol Geol*, 26: 525–528
- Fu J H, Liu Y L, Liu J, et al. 2002. Translocating system of fault block and oil-gas reservoir-forming pattern of Linnan area (in Chinese). *Petrol Geol Reco Effi*, 3: 55–58
- Gao X Z, Du Y M, Zhang B S. 2003. The sealing of Xiakou fault and its model of controlling on the petroleum accumulation (in Chinese). *Petrol Explor Dev*, 30: 76–78
- Han T Y, Qi J F, Lin H X. 2003. Study of Cenozoic tectonic evolution and hydrocarbon accumulation in southwest gentle slope belt, Huimin sag (in Chinese). *Oil Gas Geol*, 24: 245–248
- Hanson R S, Hanson T E. 1996. Methanotrophic bacteria. *Microbiol Rev*, 60: 439

- Heroy W B. 1969. *Unconventional Methods in Exploration for Petroleum and Natural Gas*. Dallas: Southern Methodist University Press. 205–218
- Hopmans E C, Schouten S, Pancost R D, et al. 2000. Analysis of intact tetraether lipids in archaeal cell material and sediments by high performance liquid chromatography/atmospheric pressure chemical ionization mass spectrometry. *Rapid Comm Mass Spectr*, 14: 585–589
- Hu G Q, Zhang H, Deng Y, et al. 2006. Application of microbial technique in prospecting for oil and gas (in Chinese). *Chin J Appl Environ Biol*, 12: 824–827
- Huguet C, Kim J-H, Sinninghe Damsté J S, et al. 2006. Reconstruction of sea surface temperature variations in the Arabian Sea over the last 23 kyr using organic proxies (TEX<sub>86</sub> and U<sub>37</sub><sup>K</sup>). *Paleoceanography*, 21: 1–13
- Jia G X. 2000. The influence factors of soil integrated oil and gas geochemical anomalies (in Chinese). *Min Resour Geol*, 14: 551–555
- Jiang T, Ren C, Xia X H. 2003. The experimental research on the occurrence modes and geochemical indices of oil-gas micropercolated hydrocarbon in near-surface soil (in Chinese). *Geophys Geochem Explor*, 27: 251–254
- Matthew M D. 1996. Importance of sampling design and density in target recognition. *Hydrocarbon migration and its near surface expression*. AAPG Memoir, 66: 24
- Mei B W, Yuan Z H. 2004. Application of geo-microbiological techniques to oil and gas exploration and development (in Chinese). *Nat Gas Geosci*, 15: 156–161
- Ménot G, Bard E, Rostek F, et al. 2006. Early reactivation of European rivers during the last Deglaciation. *Science*, 313: 1623–1625
- Schouten S, Eldrett J, Greenwood D R, et al. 2008. Onset of long-term cooling of Greenland near the Eocene-Oligocene boundary as revealed by branched tetraether lipids. *Geology*, 36: 147–150
- Schouten S, Hopmans E C, Sinninghe Damsté J S. 2013. The organic geochemistry of glycerol dialkyl glycerol tetraether lipids: A review. *Org Geochem*, 54: 19–61
- Nazina T N. 2000. Diversity and activity of microorganisms in the Daqing Oil Field of China and their potential for biotechnological applications. *Res Environ Biotechnol*, 69: 161–172
- Ning F X. 2008. Activity analysis of Xiakou fault and its effect on the petroleum (in Chinese). *Sci Technol Innov Her*, 8: 116–117
- Saunders D F, Burson K R, Thompson C K. 1999. Model for hydrocarbon microseepage and related near-surface alterations. *AAPG Bull.* 83: 170–185
- Schumacher D. 1999. *Treatise of petroleum geology/handbook of petroleum geology: Exploring for oil and gas traps*. AAPG (Spec Vol): 18–1–18–27
- Sinninghe Damsté J S, Rijpstra W I C, Hopmans E C, et al. 2011. 13,16-Dimethyl octacosanedioic acid (isodiaboloic acid), a common membrane spanning lipid of acidobacteria subdivisions 1 and 3. *Appl Environ Microbiol*, 77: 4147–4154
- Sun Q, Chu G Q, Liu M M, et al. 2011. Distributions and temperature dependence of branched glycerol dialkyl glycerol tetraethers in recent lacustrine sediments from China and Nepal. *J Geophys Res*, 116: 1–12
- Weijers J W H, Schouten S, van der Donker J C, et al. 2007a. Environmental controls on bacterial tetraether membrane lipid distribution in soils. *Geochim Cosmochim Acta*, 71: 703–713
- Weijers J W H, Schefuß E, Schouten S, et al. 2007b. Coupled thermal and hydrological evolution of tropical Africa over the last deglaciation. *Science*, 315: 1701–1704
- Weijers J W H, Schouten S, Sluijs A, et al. 2007c. Warm Arctic continents during the Palaeocene–Eocene thermal maximum. *Earth Planet Sci Lett*, 261: 230–238
- Weijers J W H, Panoto E, van Bleijswijk J, et al. 2009. Constraints on the biological source(s) of the orphan branched tetraether membrane lipids. *Geomicrobiol J*, 26: 402–414
- Wu C Z. 2005. Microbial oil and gas exploration technique and its application (in Chinese). *Nat Gas Geosci*, 16: 82–87
- Yang H, Yang H, Ding W H, et al. 2012. Soil pH impact on microbial tetraether lipids and terrestrial input index (BIT) in China. *Sci China Earth Sci*, 55: 236–245
- Yuan Z H, Mei B W, She Y H, et al. 2002. Application of microbial prospecting technology to oil and gas exploration in Xiliu area (in Chinese). *Acta Petrol Sin*, 23: 29–32
- Zhao M F, Liu Z R, Xin Q L, et al. 2000. Fault activity features and its control over oil of Linnan area in Huimin depression (in Chinese). *Petrol Explor Dev*, 27: 9–11
- Zhu Z Q, Gao X Z, Zeng J H. 2009. Fault sealing of south-west gentle slope belt in Huimin depression (in Chinese). *J China Univ Petrol*, 33: 1–5